TECHNISCHE UNIVERSITÄT CHEMNITZ

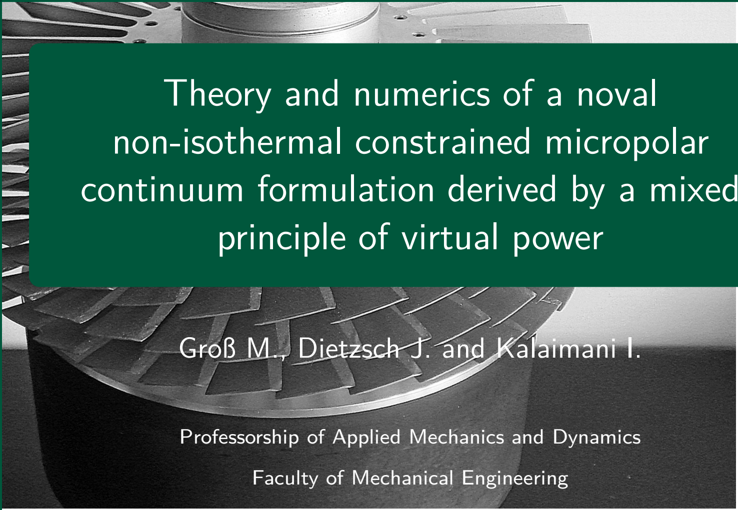

Theory and numerics of a noval non-isothermal constrained micropolar continuum formulation derived by a mixed principle of virtual power

Groß M., Dietzsch J. and Kalaimani I.

Professorship of Applied Mechanics and Dynamics

Faculty of Mechanical Engineering

ACEX 2021 (hybrid event) 04-08 July, 2021

Acknowledgment: This research is provided by DFG under the grant GR 3297

Motivation: roving-matrix composite simulation

Background: Roving-matrix composite parts in rotordynamics

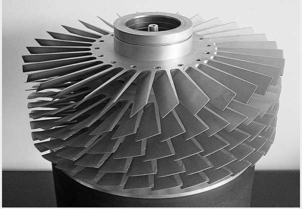

Kai Uhlig [2017] (IPF TU Dresden), recommended by IST TU Chemnitz

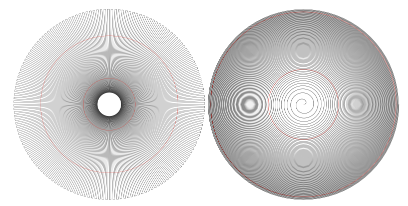

Kai Uhlig [2017]

Modelling: The need for macroscopic formulations with length scales

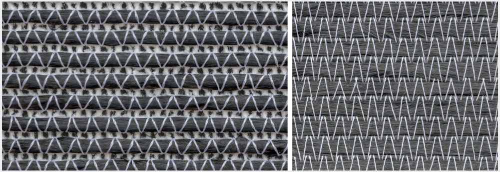

Kai Uhlig [2017]

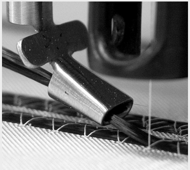

Kai Uhlig [2017]

Goal: FEM taking into account length scales in anisotropic continuum formulations

We design dynamic mixed FE methods for higher gradient materials with length scales

Overview about gradient material formulations

(see e.g. Spencer & Soldatos [2007], Askes & Aifantes [2011], Madeo et al. [2015], Asmanoglo & Menzel [2017], Ferretti et al. [2014])

Mindlin's theory of gradient elasticity (see e.g. Mindlin [1964], Askes & Aifantes [2011])

- Continua with microstructure
  - multi-scale formulations
    - macroscopic displacement
    - gradient of macro-displacement
    - microscopic deformation tensor
    - gradient of micro-deformation
  - mono-scale formulations
    - macroscopic displacement vector
    - gradient of
      - macro-displacement
      - macroscopic strain
      - macroscopic rotation

Modelling of fiber-reinforced materials (see e.g. Reese, Raible & Wriggers [2001])

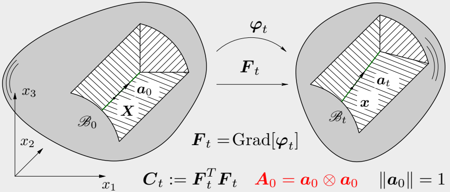

$\boldsymbol{F}_t = \mathrm{Grad}[\boldsymbol{\varphi}_t]$

$\boldsymbol{C}_t := \boldsymbol{F}_t^T \boldsymbol{F}_t \quad \boldsymbol{A}_0 = \boldsymbol{a}_0 \otimes \boldsymbol{a}_0 \quad \|\boldsymbol{a}_0\| = 1$

Anisotropic gradient material models

1. $\boldsymbol{G}_t := \mathrm{Grad}[\boldsymbol{a}_t]$
   Asmanoglo & Menzel [2017]
2. $\boldsymbol{\Xi}_t := \mathrm{Grad}[\boldsymbol{C}_t]$
   Ferretti et al. [2014]
3. $\boldsymbol{G}_{\alpha_t} := \mathrm{Grad}[\boldsymbol{\alpha}_t]$

Theory and numerics of a noval non-isothermal constrained micropolar continuum formulation derived by a mixed principle of virtual power

Groß M., Dietzsch J. and Kalaimani I.

Principle of virtual power and time integration

Application example: Quasi-static analysis with dynamic load

Path-independent time integration (motivated by Betsch & Steinmann [2002], Armero [2008])

1. Preservation of balance law of potential energy

$$\boxed{\mathcal{H}_t := \Pi^{\text{int}}(\boldsymbol{C}_t) + \Pi^{\text{ext}}(\boldsymbol{\varphi}_t, \boldsymbol{C}_t)}$$

$$\mathcal{H}_{t_{n+1}} - \mathcal{H}_{t_n} = \int_{t_n}^{t_{n+1}} \left\{ \int_{\mathscr{B}_0} \frac{\partial \Psi}{\partial \boldsymbol{C}_t} : \dot{\boldsymbol{C}}_t \, \mathrm{d}V \, \mathrm{d}t + \left[\int_{\partial_T \mathscr{B}_0} \bar{\boldsymbol{T}}(t) \cdot \dot{\boldsymbol{\varphi}}_t \, \mathrm{d}A + \frac{1}{2} \int_{\mathscr{B}_0} \bar{\boldsymbol{S}}(t) : \dot{\boldsymbol{C}}_t \, \mathrm{d}V \right] \right\} \mathrm{d}t$$

2. Algorithmic stress $\bar{\boldsymbol{S}}(t)$ corrects a material non-linearity in $\Psi(\boldsymbol{Y}_1, \ldots, \boldsymbol{Y}_n)$

3. Independent time evolution variables $\tilde{\boldsymbol{Y}}_i$ correct geometric non-linearities in $\boldsymbol{Y}_i$

$$\Pi^{\text{int}}_{t_{n+1}} - \Pi^{\text{int}}_{t_n} = \int_{t_n}^{t_{n+1}} \dot{\Pi}^{\text{int}} \left(\dot{\tilde{\boldsymbol{Y}}}_1, \ldots, \dot{\tilde{\boldsymbol{Y}}}_n \right) \mathrm{d}t - \sum_{i=1}^{n} \int_{t_n}^{t_{n+1}} \int_{\mathscr{B}_0} \tilde{\boldsymbol{Z}}_i \odot \left[\dot{\tilde{\boldsymbol{Y}}}_i - \dot{\boldsymbol{Y}}_i \right] \mathrm{d}V \, \mathrm{d}t$$

Mixed principle of virtual power (cf. Schröder & Kuhl [2015])

$$\boxed{\int_{t_n}^{t_{n+1}} \delta_* \dot{\mathcal{H}} \left(\dot{\boldsymbol{\varphi}}_t, \dot{\tilde{\boldsymbol{C}}}_t, \tilde{\boldsymbol{S}}_t \right) \mathrm{d}t = 0}$$

with $\dot{\Pi}^{\text{int}} := \int_{\mathscr{B}_0} \left\{ \dot{\Psi}(\tilde{\boldsymbol{C}}_t) - \frac{1}{2} \tilde{\boldsymbol{S}}_t : \left[\dot{\tilde{\boldsymbol{C}}}_t - \overline{\boldsymbol{F}_t^T \boldsymbol{F}_t}^{\boldsymbol{\cdot}} \right] \right\} \mathrm{d}V$

Space-time weak forms

$$\int_{t_n}^{t_{n+1}} \int_{\mathscr{B}_0} \delta_* \dot{\tilde{\boldsymbol{C}}}_t : \left[2 \frac{\partial \Psi}{\partial \tilde{\boldsymbol{C}}_t} + \bar{\boldsymbol{S}}(t) - \tilde{\boldsymbol{S}}_t \right] \mathrm{d}V \, \mathrm{d}t = 0 = \int_{t_n}^{t_{n+1}} \int_{\mathscr{B}_0} \delta_* \tilde{\boldsymbol{S}}_t : \frac{1}{2} \left[\dot{\tilde{\boldsymbol{C}}}_t - \overline{\boldsymbol{F}_t^T \boldsymbol{F}_t}^{\boldsymbol{\cdot}} \right] \mathrm{d}V \, \mathrm{d}t$$

$$\int_{t_n}^{t_{n+1}} \int_{\mathscr{B}_0} \boldsymbol{F}_t \tilde{\boldsymbol{S}}_t : \mathrm{Grad}[\delta_* \dot{\boldsymbol{\varphi}}_t] \, \mathrm{d}V \, \mathrm{d}t = \int_{t_n}^{t_{n+1}} \int_{\partial_T \mathscr{B}_0} \bar{\boldsymbol{T}}(t) \cdot \delta_* \dot{\boldsymbol{\varphi}}_t \, \mathrm{d}A \, \mathrm{d}t$$

TECHNISCHE UNIVERSITÄT CHEMNITZ

Anisotropy with rotational degrees of freedom

Theory and numerics of a noval non-isothermal constrained micropolar continuum formulation derived by a mixed principle of virtual power

Groß M., Dietzsch J. and Kalaimani I.

Anisotropy with length scales instead of meso-scale model

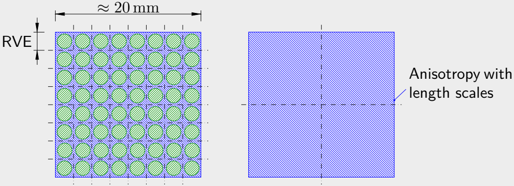

Local rotational degrees of freedom

1. Roving rotation from vorticity vector (perfect roving-matrix interface)

$$2\,\mathbb{I}^{\mathrm{skw}} := \boldsymbol{\epsilon}\cdot\boldsymbol{\epsilon} \qquad \boxed{\mathbb{I}^{\mathrm{skw}} : \boldsymbol{l}_t = -\boldsymbol{\epsilon}\cdot\boldsymbol{\omega}_t} \qquad \boldsymbol{l}_t := \dot{\boldsymbol{F}}_t\boldsymbol{F}_t^{-1} \qquad \dot{\boldsymbol{\gamma}}_t := \boldsymbol{\omega}_t$$

2. Variational setting by a rotational energy functional

$$\dot{\Pi}_{\mathrm{rot}}(\dot{\boldsymbol{\varphi}}_t, \dot{\boldsymbol{\alpha}}_t, \dot{\boldsymbol{C}}_t, \tilde{\boldsymbol{S}}_t, \tilde{\boldsymbol{\tau}}_{\mathrm{skw}}) := \dot{\Pi}^{\mathrm{int}}_{\mathrm{rot}}(\dot{\boldsymbol{C}}, \dot{\boldsymbol{\alpha}}_t) + \int_{\mathscr{B}_0} \tilde{\boldsymbol{\tau}}^T_{\mathrm{skw}} : \boldsymbol{\epsilon}\cdot\left[\frac{1}{2}\boldsymbol{\epsilon} : \dot{\boldsymbol{F}}_t\boldsymbol{F}_t^{-1} + \dot{\boldsymbol{\alpha}}_t\right] \mathrm{d}V$$

Modified/additional space-time weak forms in the quasi-static case

$$\int_{t_n}^{t_{n+1}}\int_{\mathscr{B}_0}\left[\boldsymbol{F}_t\,\tilde{\boldsymbol{S}}_t(\boldsymbol{\varphi}_t, \boldsymbol{\alpha}_t) + \tilde{\boldsymbol{\tau}}^T_{\mathrm{skw}} : \mathbb{I}^{\mathrm{skw}}\cdot\boldsymbol{F}_t^{-T}\right] : \mathrm{Grad}[\delta_*\dot{\boldsymbol{\varphi}}_t]\,\mathrm{d}V\,\mathrm{d}t = \int_{t_n}^{t_{n+1}}\int_{\partial_T\mathscr{B}_0}\bar{\boldsymbol{T}}(t)\cdot\delta_*\dot{\boldsymbol{\varphi}}_t\,\mathrm{d}A\,\mathrm{d}t$$

$$\int_{t_n}^{t_{n+1}}\int_{\mathscr{B}_0}\delta_*\tilde{\boldsymbol{\tau}}^T_{\mathrm{skw}} : \boldsymbol{\epsilon}\cdot\left[\frac{1}{2}\boldsymbol{\epsilon} : \dot{\boldsymbol{F}}_t\boldsymbol{F}_t^{-1} + \dot{\boldsymbol{\alpha}}_t\right]\mathrm{d}V\,\mathrm{d}t = 0 = \int_{t_n}^{t_{n+1}}\int_{\mathscr{B}_0}\left[\frac{\partial\Psi}{\partial\boldsymbol{\alpha}_t} + \tilde{\boldsymbol{\tau}}^T_{\mathrm{skw}} : \boldsymbol{\epsilon}\right]\cdot\delta_*\dot{\boldsymbol{\alpha}}_t\,\mathrm{d}V\,\mathrm{d}t$$

Kinematics with rotational degrees of freedom

Configurations (motivated by Wriggers [2008])

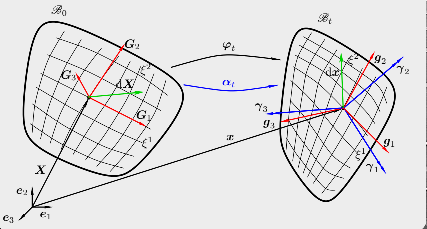

Curvilinear setting

1. Deformation mapping

$$\frac{\partial \boldsymbol{\varphi}(\boldsymbol{X}(\boldsymbol{\xi}),t)}{\partial \xi^j} =: \boldsymbol{g}_j$$

2. Rotation mapping

$$\frac{\partial \boldsymbol{\alpha}(\boldsymbol{X}(\boldsymbol{\xi}),t)}{\partial \xi^j} =: \boldsymbol{\gamma}_j$$

$$\boldsymbol{\gamma}_j := \alpha^k_{,j}\, \boldsymbol{g}_k$$

Covariant formulation (cf. Eringen [1967])

1. Metric coefficients for translations and local rotations

$$g_{ij} := \boldsymbol{g}_i \cdot \boldsymbol{g}_j \qquad \boldsymbol{g}_j = g_{ij}\, \boldsymbol{g}^i \qquad K_{ij} := \boldsymbol{g}_i \cdot \boldsymbol{\gamma}_j \qquad \boldsymbol{\gamma}_j = K_{ij}\, \boldsymbol{g}^i$$

2. Deformation/rotation gradient

$$\boldsymbol{F} = \frac{\partial \boldsymbol{\varphi}}{\partial \boldsymbol{X}} = \boldsymbol{g}_j \otimes \boldsymbol{G}^j \qquad \boldsymbol{g}_j = \boldsymbol{F}\, \boldsymbol{G}_j \qquad \boldsymbol{G}_\alpha = \frac{\partial \boldsymbol{\alpha}}{\partial \boldsymbol{X}} = \boldsymbol{\gamma}_j \otimes \boldsymbol{G}^j \qquad \boldsymbol{\gamma}_j = \boldsymbol{G}_\alpha\, \boldsymbol{G}_j$$

3. Line stretch and local curvature-twist

$$\mathrm{d}\boldsymbol{x} \cdot \boldsymbol{g} \cdot \mathrm{d}\boldsymbol{x} = \boldsymbol{dX} \cdot \boldsymbol{C} \cdot \mathrm{d}\boldsymbol{X} \qquad \boxed{\boldsymbol{C} = \boldsymbol{F}^T \boldsymbol{g} \boldsymbol{F}} \qquad \mathrm{d}\boldsymbol{x} \cdot \boldsymbol{g}_\alpha \cdot \mathrm{d}\boldsymbol{x} = \boldsymbol{dX} \cdot \boldsymbol{K} \cdot \mathrm{d}\boldsymbol{X} \qquad \boxed{\boldsymbol{K} = \boldsymbol{F}^T \boldsymbol{g}_\alpha \boldsymbol{F}}$$

4. Metric tensors

$$\boldsymbol{g} := \frac{\partial \boldsymbol{\varphi}}{\partial \boldsymbol{x}} \equiv \boldsymbol{g}_j \otimes \boldsymbol{g}^j = g_{ij}\, \boldsymbol{g}^i \otimes \boldsymbol{g}^j \qquad \boldsymbol{g}_\alpha := \frac{\partial \boldsymbol{\alpha}}{\partial \boldsymbol{x}} \equiv \boldsymbol{\gamma}_j \otimes \boldsymbol{g}^j = K_{ij}\, \boldsymbol{g}^i \otimes \boldsymbol{g}^j$$

Covariant kinematics of roving deformations

Roving curvature-twist (cf. Stokes [2012])

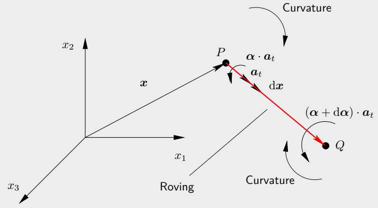

Transverse isotropy

1. Roving direction vectors

$$\boldsymbol{a}_0 = a^i\, \boldsymbol{G}_i \qquad \boldsymbol{a}_t = a^i\, \boldsymbol{g}_i$$

2. Roving deformation gradient

$$\boldsymbol{a}_t = \boldsymbol{F}_F\, \boldsymbol{a}_0 \qquad \boldsymbol{F}_F := \boldsymbol{a}_t \otimes \boldsymbol{a}_0$$

$$\boldsymbol{F}_F = \boldsymbol{F}\, \boldsymbol{A}_0$$

Deformation measures of the rovings with respect to the matrix

$$\boldsymbol{a}_t \cdot \boldsymbol{g} \cdot \mathrm{d}\boldsymbol{x} = \mathrm{d}\boldsymbol{X} \cdot \boldsymbol{C}_A \cdot \mathrm{d}\boldsymbol{X} \qquad \boxed{\boldsymbol{C}_A := \boldsymbol{A}_0\, \boldsymbol{C}}$$

$$\boldsymbol{a}_t \cdot \boldsymbol{g}_\alpha \cdot \mathrm{d}\boldsymbol{x} = \mathrm{d}\boldsymbol{X} \cdot \boldsymbol{K}_F \cdot \mathrm{d}\boldsymbol{X} \qquad \boxed{\boldsymbol{K}_F := \boldsymbol{A}_0\, \boldsymbol{K}}$$

Tensor invariants as roving deformation indicators

1. Translational deformation indicators for stretch and distorsion

$$I_1(\boldsymbol{C}_A) := \boldsymbol{C}_A : \boldsymbol{G}^{-1} \equiv I_4(\boldsymbol{C}, \boldsymbol{a}_0) \qquad J_2(\boldsymbol{C}_A) := \boldsymbol{C}_A : \boldsymbol{C}_A \equiv J_5(\boldsymbol{C}, \boldsymbol{a}_0)$$

2. Rotational deformation indicators for twist and curvature (bending)

$$I_1(\boldsymbol{K}_F) := \boldsymbol{K}_F : \boldsymbol{G}^{-1} =: T_F \qquad J_2(\boldsymbol{K}_F) := \boldsymbol{K}_F : \boldsymbol{K}_F =: \frac{B_F}{2}$$

Consistent time integration of the local rotations

Path-independence with linear stress (geometric non-linearity)

$$\dot{\Pi}_{\text{rot}}^{\text{con}} := \dot{\Pi}_{\text{rot}} + \int_{\mathscr{B}_0} \frac{\partial \Psi_K}{\partial \tilde{\boldsymbol{K}}_t} : \dot{\tilde{\boldsymbol{K}}}_t \, \mathrm{d}V - \int_{\mathscr{B}_0} \tilde{\boldsymbol{S}}_{K_t} : \left[\dot{\tilde{\boldsymbol{K}}}_t - \overline{\boldsymbol{F}_t^T \boldsymbol{G}_{\alpha_t}}^{\boldsymbol{\cdot}} \right] \mathrm{d}V$$

Path-independence with non-linear stress (material non-linearity)

$$\dot{\Pi}_{\text{rot}}^{\text{ext}}(\dot{\boldsymbol{\alpha}}_t, \dot{\boldsymbol{K}}_t) := \int_{\partial_W \mathscr{B}_0} \bar{\boldsymbol{W}}(t) \cdot \dot{\boldsymbol{\alpha}} \, \mathrm{d}A + \int_{\mathscr{B}_0} \bar{\boldsymbol{S}}_K(t) : \dot{\tilde{\boldsymbol{K}}}_t \, \mathrm{d}V$$

Modified/additional weak forms in the quasi-static case

$$\int_{t_n}^{t_{n+1}} \int_{\mathscr{B}_0} \left[\boldsymbol{F}_t \tilde{\boldsymbol{S}}_t + \boldsymbol{G}_{\alpha_t} \tilde{\boldsymbol{S}}_{K_t}^T + \tilde{\boldsymbol{\tau}}_{\text{skw}}^T : \mathbb{I}^{\text{skw}} \cdot \boldsymbol{F}_t^{-T} \right] : \mathrm{Grad}[\delta_* \dot{\boldsymbol{\varphi}}_t] \, \mathrm{d}V \, \mathrm{d}t = \int_{t_n}^{t_{n+1}} \int_{\partial_T \mathscr{B}_0} \bar{\boldsymbol{T}}(t) \cdot \delta_* \dot{\boldsymbol{\varphi}}_t \, \mathrm{d}A \, \mathrm{d}t$$

$$\int_{t_n}^{t_{n+1}} \int_{\mathscr{B}_0} \boldsymbol{F}_t \tilde{\boldsymbol{S}}_{K_t} : \mathrm{Grad}\left[\delta_* \dot{\boldsymbol{\alpha}}_t\right] \mathrm{d}V \, \mathrm{d}t + \int_{t_n}^{t_{n+1}} \int_{\mathscr{B}_0} \tilde{\boldsymbol{\tau}}_{\text{skw}}^T : \boldsymbol{\epsilon} \cdot \delta_* \dot{\boldsymbol{\alpha}}_t \, \mathrm{d}V \, \mathrm{d}t = \int_{t_n}^{t_{n+1}} \int_{\partial_W \mathscr{B}_0} \bar{\boldsymbol{W}}(t) \cdot \delta_* \dot{\boldsymbol{\alpha}}_t \, \mathrm{d}A \, \mathrm{d}t$$

$$\int_{t_n}^{t_{n+1}} \int_{\mathscr{B}_0} \delta_* \dot{\tilde{\boldsymbol{K}}}_t : \left[\frac{\partial \Psi_K}{\partial \tilde{\boldsymbol{K}}_t} + \bar{\boldsymbol{S}}_K(t) - \tilde{\boldsymbol{S}}_{K_t} \right] \mathrm{d}V \, \mathrm{d}t = 0 = \int_{t_n}^{t_{n+1}} \int_{\mathscr{B}_0} \delta_* \tilde{\boldsymbol{S}}_{K_t} : \left[\dot{\tilde{\boldsymbol{K}}}_t - \overline{\boldsymbol{F}_t^T \boldsymbol{G}_{\alpha_t}}^{\boldsymbol{\cdot}} \right] \mathrm{d}V \, \mathrm{d}t$$

Material and two-point stress tensors

$$\boldsymbol{S}_K := \frac{\partial \Psi_K}{\partial \boldsymbol{K}} \qquad \boldsymbol{N}_K := \boldsymbol{G}_\alpha \boldsymbol{S}_K^T \qquad \boldsymbol{P}_K := \boldsymbol{F} \boldsymbol{S}_K$$

'Spatial' stress tensors

$$\boldsymbol{\tau}_K^T := \boldsymbol{F} \boldsymbol{N}_K^T \qquad \boldsymbol{\mu}_K := \boldsymbol{P}_K \boldsymbol{F}^T$$

Path-independence couple stress approximation

Path-independence relation for local rotations

$$\Psi_K(\tilde{\boldsymbol K}_{t_{n+1}}) - \Psi_K(\tilde{\boldsymbol K}_{t_n}) = \int_{t_n}^{t_{n+1}} \dot{\Psi}_K(\tilde{\boldsymbol K}_t)\,\mathrm{d}t \equiv \int_0^1 \overset{\circ}{\Psi}_K(\tilde{\boldsymbol K}_\alpha)\,\mathrm{d}\alpha$$

Separate constrained variational problem for 'system input' $\bar{\boldsymbol S}_K(\alpha)$

$$\mathcal{F}_K(\bar{\boldsymbol S}_K(\alpha), \lambda_K) := \lambda_K\,\mathcal{G}_K(\bar{\boldsymbol S}_K(\alpha)) + \int_0^1 F_K(\bar{\boldsymbol S}_K(\alpha))\,\mathrm{d}\alpha \overset{!}{=} \text{extr}$$

Path independence condition as local stress constraint

$$\mathcal{G}_K(\bar{\boldsymbol S}_K(\alpha)) := \Psi_K(\tilde{\boldsymbol K}_{t_{n+1}}) - \Psi_K(\tilde{\boldsymbol K}_{t_n}) - \int_0^1 \left[\bar{\boldsymbol S}_K(\alpha) + \frac{\partial \Psi_K(\tilde{\boldsymbol K}_\alpha)}{\partial \tilde{\boldsymbol K}_\alpha}\right] : \overset{\circ}{\tilde{\boldsymbol K}}_\alpha\,\mathrm{d}\alpha$$

Minimization function

$$F_K(\bar{\boldsymbol S}_K(\alpha)) := \frac{1}{2}\,\boldsymbol g\,\bar{\boldsymbol\mu}_K : \bar{\boldsymbol\mu}_K\,\boldsymbol g \equiv \frac{1}{2}\,\boldsymbol C_\alpha\,\bar{\boldsymbol S}_K(\alpha) : \bar{\boldsymbol S}_K(\alpha)\,\boldsymbol C_\alpha$$

Algorithmic couple stress tensor

$$\bar{\boldsymbol S}_K(\alpha) := \lambda_K\,\tilde{\boldsymbol C}_\alpha^{-1}\,\overset{\circ}{\tilde{\boldsymbol K}}_\alpha\,\tilde{\boldsymbol C}_\alpha^{-1}$$

Couple stress multiplier

$$\lambda_K = \frac{\mathcal{G}_K(\boldsymbol O)}{\int_0^1 \tilde{\boldsymbol C}_\alpha^{-1}\,\overset{\circ}{\tilde{\boldsymbol K}}_\alpha : \overset{\circ}{\tilde{\boldsymbol K}}_\alpha\,\tilde{\boldsymbol C}_\alpha^{-1}\,\mathrm{d}\alpha}$$

Dynamical formulation with inertia effects

Total energy with kinetic energy from local rotations

$$\mathcal{H} := \mathcal{T}^{\mathrm{tra}} + \mathcal{T}^{\mathrm{rot}} + \Pi^{\mathrm{int}}$$

Total kinetic energy

1. Translational kinetic energy

$$\mathcal{T}^{\mathrm{tra}}(\dot{\boldsymbol{\varphi}}, \boldsymbol{v}, \boldsymbol{p}) := \frac{1}{2}\int_{\mathscr{B}_0} \boldsymbol{v} \cdot [\rho_0\, \boldsymbol{I}]\, \boldsymbol{v}\, \mathrm{d}V - \int_{\mathscr{B}_0} [\boldsymbol{v} - \dot{\boldsymbol{\varphi}}] \cdot \boldsymbol{p}\, \mathrm{d}V$$

2. Rotational kinetic energy

$$\mathcal{T}^{\mathrm{rot}}(\dot{\boldsymbol{\alpha}}, \boldsymbol{\omega}, \boldsymbol{\pi}) := \frac{1}{2}\int_{\mathscr{B}_0} \boldsymbol{\omega} \cdot \boldsymbol{J}\boldsymbol{\omega}\, \mathrm{d}V - \int_{\mathscr{B}_0} [\boldsymbol{\omega} - \dot{\boldsymbol{\alpha}}] \cdot \boldsymbol{\pi}\, \mathrm{d}V$$

RVE with roving

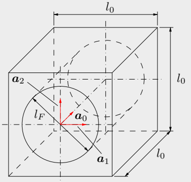

Inertia density tensor of a roving (cf. Zhilin [2000])

1. Inertia density in the RVE coordinate system

$$\boldsymbol{J} = J_F\, \boldsymbol{a}_0 \otimes \boldsymbol{a}_0 + J_1\, \boldsymbol{a}_1 \otimes \boldsymbol{a}_1 + J_2\, \boldsymbol{a}_2 \otimes \boldsymbol{a}_2$$

2. Transverse isotropy ($J_1 = J_2 =: \rho_0\,(l_0)^2$)

$$\boxed{\boldsymbol{J} = \rho_0\,(l_F)^2\, \boldsymbol{A}_0 + \rho_0\,(l_0)^2\,[\boldsymbol{I} - \boldsymbol{A}_0]}$$

$$\boldsymbol{a}_1 \otimes \boldsymbol{a}_1 + \boldsymbol{a}_2 \otimes \boldsymbol{a}_2 = \boldsymbol{I} - \boldsymbol{A}_0 \qquad J_F := \rho_0\,(l_F)^2$$

Turbomolecular pump rotor under dynamic loads
(Boundary and initial conditions I; 121-em with H8-mixed-Bbar)

Boundary conditions on the top side

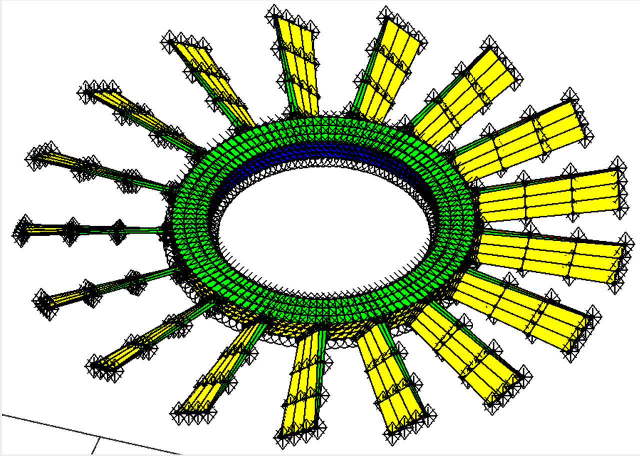

Dirichlet and Neumann boundaries on the top side

Yellow patches: cooling with fixed temperature $\Theta = \Theta_\infty = 298.15$

Green patches: insulation $\bar{Q}^A := 0$ and torque load $W_z^A = -\hat{W}^A(t)$

Turbomolecular pump rotor under dynamic loads
(Boundary and initial conditions II; 121-em with H8-mixed-Bbar)

Boundary conditions on the bottom side

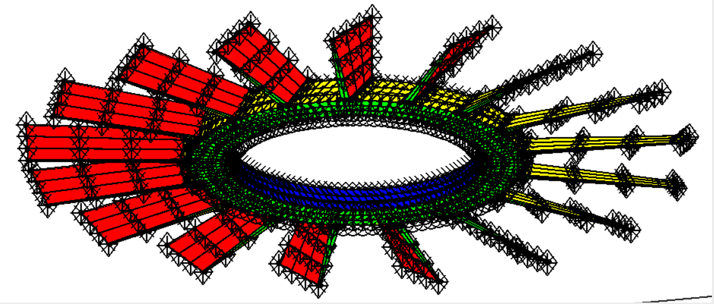

Dirichlet and Neumann boundaries on the bottom side

Blue inner patches:	fixed temperature $\Theta = \Theta_\infty$
Red front patches:	follower load and inward head $\bar{Q}^A := \hat{Q}^A(t)$
Green bottom patches:	z-dof fixed with thermal insulation $\bar{Q}^A := 0$
Green patches:	Thermal insulation $\bar{Q}^A := 0$

Initial conditions

$$\boldsymbol{\varphi}_0^A = \boldsymbol{X}^A \quad \boldsymbol{\alpha}_0^A = \mathbf{0} \quad \boldsymbol{v}_0^A = \mathbf{0} \quad \boldsymbol{\omega}_0^A = \mathbf{0} \quad \Theta_0^A = \Theta_\infty \quad \eta_0^A = 0 \quad \boldsymbol{\tau}_{\mathrm{skw}}^A = \boldsymbol{O}$$

Turbomolecular pump rotor under dynamic loads
(Roving distribution; 121-em with H8-mixed-Bbar)

Roving direction field at Gauss points in space

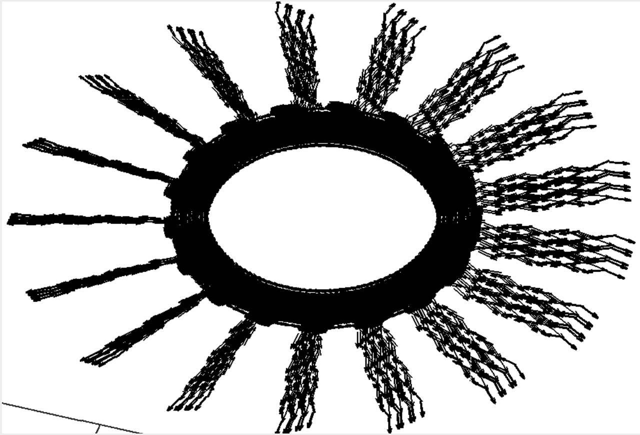

Roving direction fields

Rotor blades: two layers with diagonal rovings (crossed)
Rotor hub : rovings in tangential direction (see motivation)

Turbomolecular pump rotor under dynamic loads
(Loads and generalized reactions; 121-em with H8-mixed-Bbar)

Time evolutions of applied loads and generalized reactions

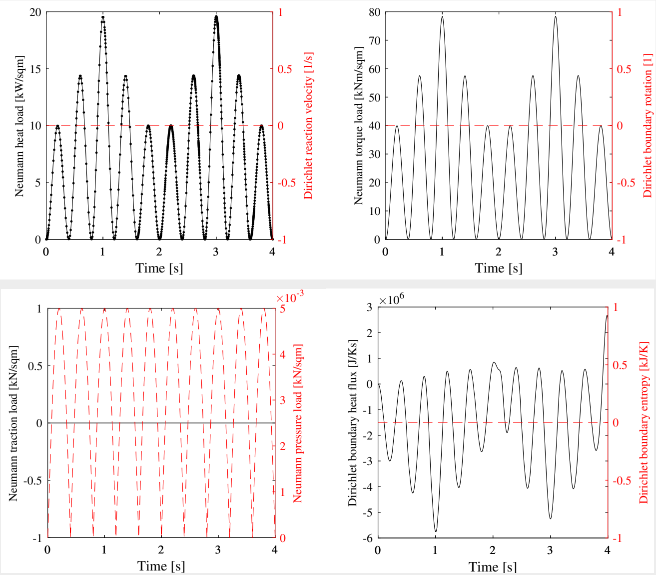

TECHNISCHE UNIVERSITÄT CHEMNITZ

Turbomolecular pump rotor under dynamic loads
(Illustration of roving deformation; hand with mouse cord)

Movie of the roving deformation

Turbomolecular pump rotor under dynamic loads
(Current configurations I; 121-em with H8-mixed-Bbar)

Movie of simulated motion with circumferential elongation as color

Turbomolecular pump rotor under dynamic loads
(Current configurations II; 121-em with H8-mixed-Bbar)

Current temperature and heat load arrows at $t_n = 3.0\,\mathrm{s}$

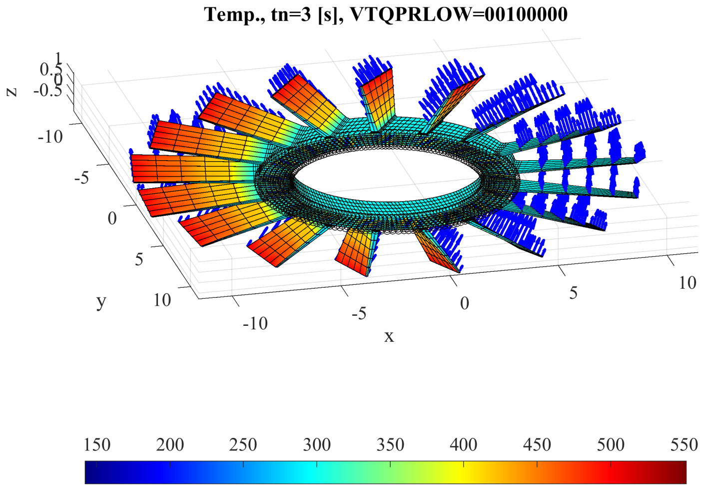

TECHNISCHE UNIVERSITÄT CHEMNITZ

Turbomolecular pump rotor under dynamic loads
(Current configurations III; 121-em with H8-mixed-Bbar)

Rate of roving bending and torque load arrows at $t_n = 2.2\,\mathrm{s}$

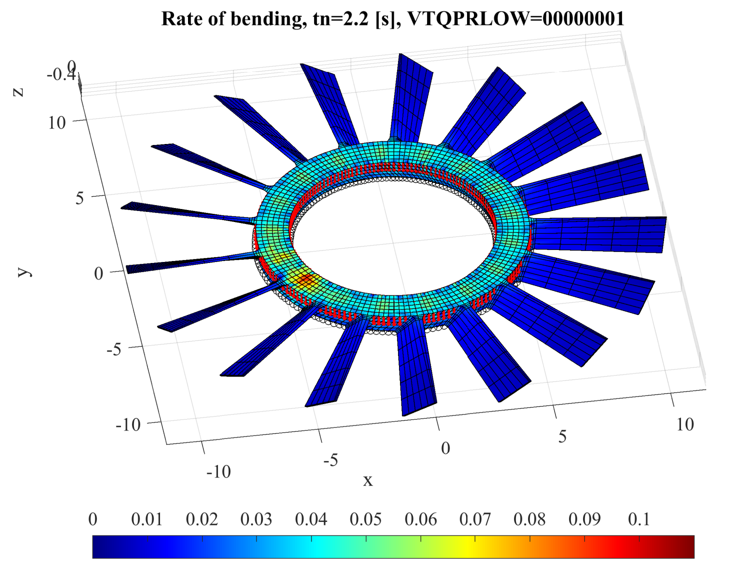

Turbomolecular pump rotor under dynamic loads
(Current configurations IV; 121-em with H8-mixed-Bbar)

Twist rate of roving and pressure load arrows at $t_n = 2.2\,\mathrm{s}$

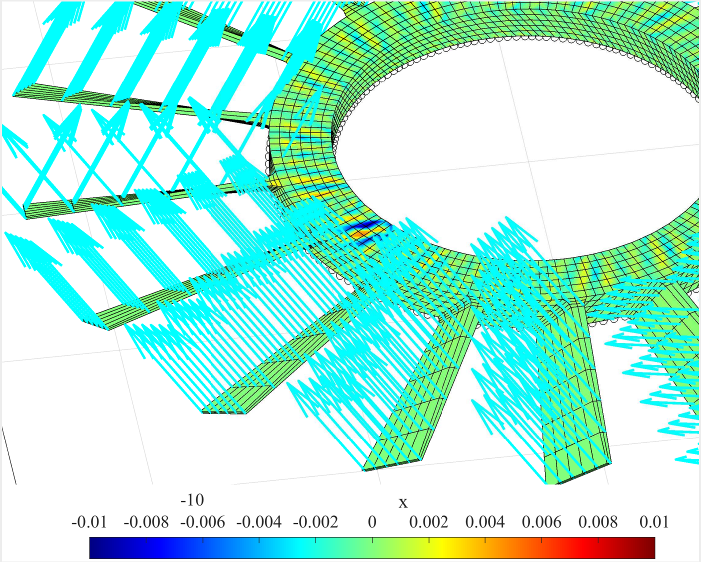

Turbomolecular pump rotor under dynamic loads
(Time evolutions I; 121-em with H8-mixed-Bbar)

Solutions over time at space node $A = 5198$

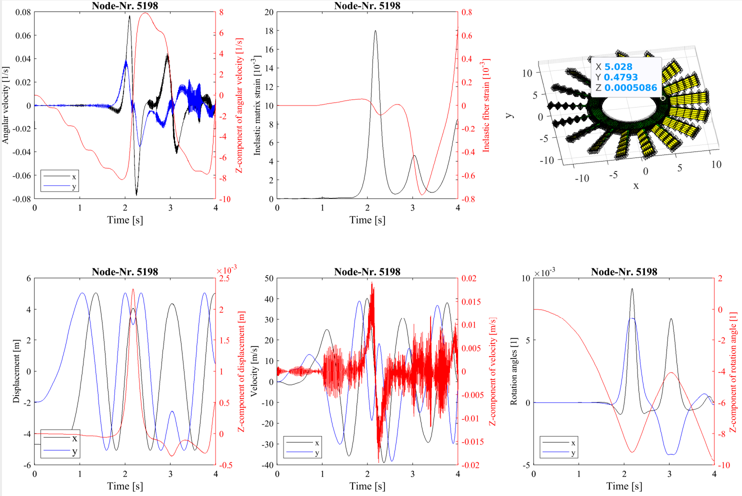

Turbomolecular pump rotor under dynamic loads
(Time evolutions II; 121-em with H8-mixed-Bbar)

Energies and momenta over time

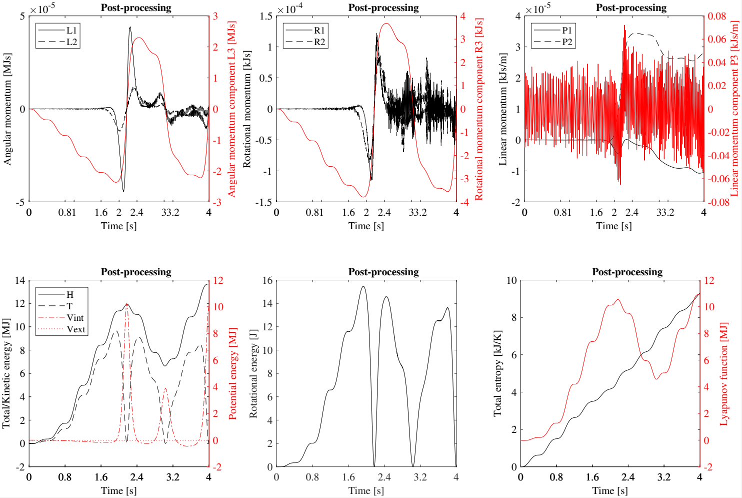

Turbomolecular pump rotor under dynamic loads
(Roving distribution radial; 121-em with H8-mixed-Bbar)

Roving direction field at Gauss points in space

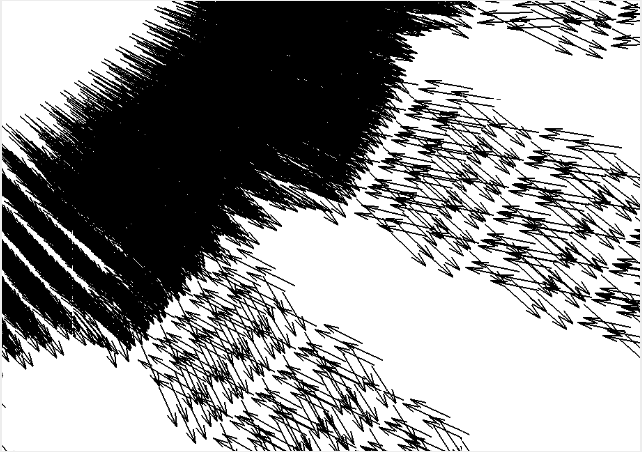

Roving direction fields

Rotor blades: two layers with diagonal rovings (crossed)
Rotor hub : rovings in radial direction (see motivation)

Turbomolecular pump rotor under dynamic loads
(Current configurations radial-I; 121-em with H8-mixed-Bbar)

Movie of simulated motion with circumferential elongation as color

Turbomolecular pump rotor under dynamic loads
(Current configurations radial-II; 121-em with H8-mixed-Bbar)

Rate of roving bending and torque load arrows at $t_n = 1.4993\,\mathrm{s}$

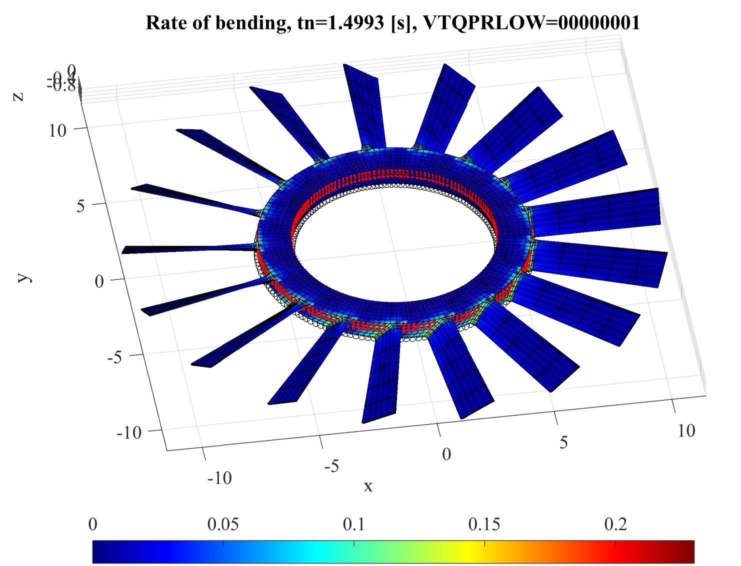

Turbomolecular pump rotor under dynamic loads
(Current configurations radial-III; 121-em with H8-mixed-Bbar)

Twist rate of roving and pressure load arrows at $t_n = 1.4993\,\mathrm{s}$

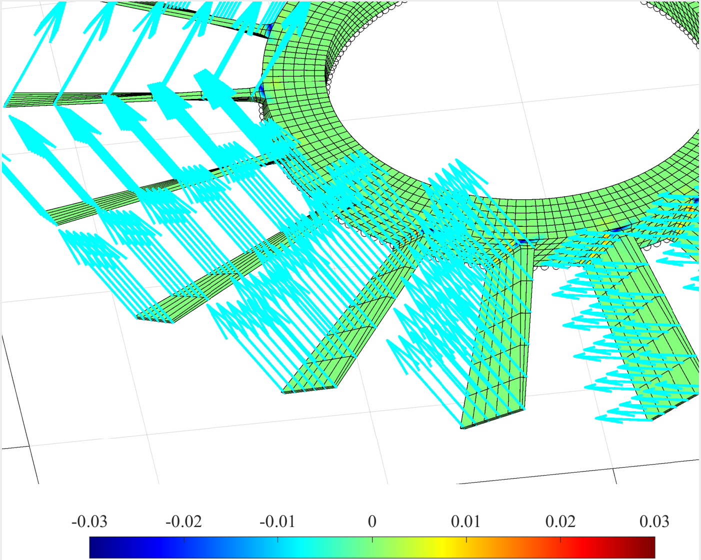

Summary

1. Motivation:
   - Dynamic finite element simulations of fiber roving composites
   - Extension of transverse isotropy with length scale parameters
2. Goals: FE simulations which
   - take into account the roving diameter and spacing,
   - roving stiffness with respect to curvature and twist.
3. Strategy:
   - Introduction of a mixed field for the gradient of rotation
   - Discretization by using a mixed principle of virtual power
4. Results: Length scales for
   - roving diameter/spacing in the kinetic energy density
   - roving torsional/flexural stiffness in the strain energy
5. Outlook:
   - Material optimization in order to reduce the start-up vibrations
   - Identification of length scale parameters using mesoscale models